

## Phase transitions in ferroelectric-paraelectric superlattices

A. P. Levanyuk and I. B. Misirlioglu

Citation: *J. Appl. Phys.* **110**, 114109 (2011); doi: 10.1063/1.3662197

View online: <http://dx.doi.org/10.1063/1.3662197>

View Table of Contents: <http://jap.aip.org/resource/1/JAPIAU/v110/i11>

Published by the [American Institute of Physics](#).

---

### Related Articles

Modeling the switching kinetics in ferroelectrics

*J. Appl. Phys.* **110**, 114106 (2011)

Ferroelectric phase transition and low-temperature dielectric relaxations in  $\text{Sr}_4(\text{La}_{1-x}\text{Sm}_x)_2\text{Ti}_4\text{Nb}_6\text{O}_{30}$  ceramics

*J. Appl. Phys.* **110**, 114101 (2011)

Poling temperature tuned electric-field-induced ferroelectric to antiferroelectric phase transition in  $0.89\text{Bi}0.5\text{Na}0.5\text{TiO}_3\text{-}0.06\text{BaTiO}_3\text{-}0.05\text{K}0.5\text{Na}0.5\text{NbO}_3$  ceramics

*J. Appl. Phys.* **110**, 094109 (2011)

Structural transitions and enhanced ferroelectricity in Ca and Mn co-doped  $\text{BiFeO}_3$  thin films

*J. Appl. Phys.* **110**, 094106 (2011)

Measurements and ab initio molecular dynamics simulations of the high temperature ferroelectric transition in hexagonal  $\text{RMnO}_3$

*J. Appl. Phys.* **110**, 084116 (2011)

---

### Additional information on J. Appl. Phys.

Journal Homepage: <http://jap.aip.org/>

Journal Information: [http://jap.aip.org/about/about\\_the\\_journal](http://jap.aip.org/about/about_the_journal)

Top downloads: [http://jap.aip.org/features/most\\_downloaded](http://jap.aip.org/features/most_downloaded)

Information for Authors: <http://jap.aip.org/authors>

### ADVERTISEMENT

**AIP**Advances

*Submit Now*

Explore AIP's new  
open-access journal

- Article-level metrics now available
- Join the conversation! Rate & comment on articles

## Phase transitions in ferroelectric-paraelectric superlattices

A. P. Levanyuk<sup>1,2,3</sup> and I. B. Misirlioglu<sup>1,a)</sup>

<sup>1</sup>*Faculty of Engineering and Natural Sciences, Sabanci University, Tuzla/Orhanli, 34956, Istanbul, Turkey*

<sup>2</sup>*Moscow Institute of Radioengineering, Electronics and Automation, Moscow 117454, Russia*

<sup>3</sup>*Departamento de Fisica de la Materia Condensada, C-III, Universidad Autonoma de Madrid, 28049 Madrid, Spain*

(Received 26 May 2011; accepted 19 October 2011; published online 5 December 2011)

Within the phenomenological Landau–Ginzburg–Devonshire theory, we discuss the paraelectric-ferroelectric transition in superstructures consisting of ferroelectric and paraelectric layers of equal thickness. The polar axis of the ferroelectric is perpendicular to the layer plane as expected in fully strained BaTiO<sub>3</sub>/SrTiO<sub>3</sub> superstructures on SrTiO<sub>3</sub> substrates with pseudomorphic electrodes. We concentrate on the electrostatic effects and do not take into account the boundary conditions other than the electrostatic ones. We find that when the ferroelectric phase transition in the superstructures is into a multidomain state, both its temperature and its character, i. e., the profile of the polarization appearing at the phase transition is strongly influenced by the nature of the near-electrode region. This is also the case for the layer thickness separating the single- and multidomain regimes of the transition. Such a finding makes us question the idea that these superstructures can be thought of as infinite systems, i.e., periodic superstructures similar to a crystal. The irrelevance of this idea in certain conditions is demonstrated by comparing the phase transitions in two different superstructures consisting of ferroelectric and paraelectric layers of the same thickness. In one of them, the ferroelectric layer is in immediate contact with an ideal metallic electrode, whereas at the other boundary, it is the paraelectric layer that is in contact with the electrode. In another superstructure, one paraelectric layer is split in two equal parts which are placed as the first and last layer between the electrodes and the ferroelectric layers which are closest to the electrodes. We show (with some formal reservations) that the phase transition temperature in the first superstructure can be over 100 °C more than in the second one if the material parameters of BaTiO<sub>3</sub>/SrTiO<sub>3</sub> are used for the estimations. Moreover, the profile of the polarization arising at the phase transition is inhomogeneous along the superstructure and has the maximum amplitude in the ferroelectric layer contacting the electrode. We argue that this situation is general and results in smearing of the phase transition anomalies for the layer thicknesses corresponding to multidomain transitions. The work is mainly analytical but numerical methods have been used to support some statements that have been put forward as hypotheses. © 2011 American Institute of Physics. [doi:10.1063/1.3662197]

### I. INTRODUCTION

Currently there is a lot of attention devoted to ferroelectric-paraelectric superlattices.<sup>1–8</sup> However, the phenomenological theory of phase transitions in these systems is still far from being complete and consistent. This may seem surprising because the theory of these systems started<sup>9–12</sup> well before the first experimental realization of the superlattices.<sup>13,14</sup> Earlier theoretical works were based on the consideration that the ferroelectric polarization was parallel to the plane of the structure. This was both natural and correct because the authors considered superlattices consisting of layers of cubic ferroelectrics with the layer plane perpendicular to a cubic axis. It was correct to expect that the ferroelectric polarization would be directed along a cubic axis parallel to the layer plane because there was no depolarizing field in this configuration. Multilayers in experimental studies do not, however, usually consist of cubic ferroelectric materials [see Refs. 1–8; because of the misfit strains, the cubic paraelectric phase transforms into (at least) a tetragonal state either with

the polar axis perpendicular to the layer plane (uniaxial ferroelectric) or with two polar axes parallel to the plane (two-axial ferroelectric)]. In this paper, we are focusing on the former, uniaxial case, which seems to be the main interest for experimental works. Because the ferroelectric polarization is perpendicular to the interface, the depolarizing field determines both the temperature and the character of the ferroelectric phase transition. Thus the non-electrostatic effects at the interface (“short-range interlayer interaction”), which was the main emphasis in Refs. 9–12, become of secondary importance. This reasonable idea was pursued in Refs. 15 and 16 in which the authors discussed one aspect of the depolarizing field: Lowering of the temperature of the ferroelectric phase transition into the single domain state, which is an effect known, in principle, since the work of Batra *et al.*<sup>17</sup> In other words, the authors took for granted that the ferroelectric phase transition was into a single domain state. There is, however, another possibility: That this transition could be into a multidomain state. It should be noted that the interplay between single- and multidomain transitions in a ferroelectric slab between metallic electrodes with two dielectric layers between the ferroelectric and the electrodes has been

<sup>a)</sup>Electronic mail: burc@sabanciuniv.edu.

discussed in some detail by Chensky and Tarasenko (ChT)<sup>18</sup> in their 1982 paper. The very same approach of ChT has been used by Stephanovich *et al.*<sup>19</sup> to discuss the ferroelectric phase transitions in multilayers of the type we are analyzing. In their work, they supposed that the spatial distribution of the ferroelectric polarization appearing as a result of the phase transition is periodic along the superstructure. This analogy with ordinary crystals looks quite natural, and it is not surprising that other research groups have adopted this assumption.<sup>19,20</sup> In our work, using the same approach as in Ref. 19, we show that the periodicity assumption along the out-of-plane direction is not justified. We consider two specific cases of superstructures. For one of them, we explicitly show that assuming periodicity may not hold regardless of the system size. For another special case, the assumption of periodicity seems to be, hypothetically, correct but this system is a very specific case.

The physical reason prohibiting the periodicity assumption is that the superstructure is never sufficiently thick to consider it as an analog of a periodic crystal. Experimentally, the lateral sizes of the electrode or external surface are always much larger than the total thickness of the superstructure. Theoretically, this corresponds to the supposition that the layers are laterally infinite. Therefore, no point or region inside of the superstructure is “sufficiently far” from the boundaries. At the same time, the structure of the boundary layers strongly influences how the depolarizing field is compensated, and this impacts the whole system. To show this, we compare the phase transitions in two different superstructures consisting of ferroelectric and paraelectric layers of the same thickness. One of these structures has the ferroelectric layer in immediate contact with an ideal metallic electrode, while at the other boundary, it is a paraelectric layer that is in contact with the electrode. We name such a stack of layers a system consisting of bilayer cells. In the other superstructure, one paraelectric layer is split in two equal parts that are situated between the electrodes and ferroelectric layers. We also name such a stack of layers starting with half a paraelectric layer contacting one electrode and ending again with half a paraelectric layer before the other electrode a system consisting of ChT cells. We were unable to rigorously analyze the phase transitions in the two systems. However, we were able to show that the phase transitions are very different both in terms of the transition temperatures and the profile of the space distribution of ferroelectric polarization arising at the transition.

The sensitivity of the phase transition to the characteristics of the near-electrode region forces us to be cautious about comparison of the experimental data with theoretical formulae for idealized models. That is why we do not try to make this comparison, although, for the sake of illustration, we use in our plots the physical parameters of BaTiO<sub>3</sub>-SrTiO<sub>3</sub> superstructures. To be able to produce results comparable to experiments, the theory should consider further developments, and we see our paper as no more than a step in this direction.

Throughout the paper we shall not take into account the non-electrostatic boundary conditions at the ferroelectric-paraelectric interfaces, similar to ChT<sup>18</sup> and unlike Stephanovich *et al.*<sup>19</sup> There is no doubt that for a realistic comparison with experiments, these conditions should be taken into

account. But this paper is devoted mainly to conceptual problems, which, as we have already mentioned, prove to be fairly difficult by themselves. That is why we prefer not to divert the reader’s attention from these conceptual problems. The only parameter that we shall try to calculate in this paper is the phase transition temperature for different total thicknesses of the pair of the layers in the superstructures. We shall also analyze the form of the polarization profile setting in at the phase transition.

The paper is organized as follows: In Sec. II, we consider small systems consisting of either two or three ferroelectric/paraelectric layers. We begin this part by describing the ChT results relevant to what is considered in this paper. Also, we apply their approach to other three or two layer systems as a preparation to analyze the systems given in the next section. In Sec. III, we try to understand what happens in large systems, considering first doubled “small systems” and then generalizing some of the results to systems of arbitrary length. The physical conclusions we arrive at using the obtained results are discussed in Sec. IV. In Sec. V, we summarize the results of our paper.

## II. SMALL SYSTEMS

### A. The Chensky and Tarasenko approach

The system ChT studied is illustrated in Fig. 1. Upon cooling, the ferroelectric phase transition in this system may be either into single or multidomain states. Naturally, when the thickness of the paraelectric (“dead”) layers is sufficiently small, the transition will be into single domain state. ChT calculated the maximum dead layer thickness ( $d_c$ ) for this phase transition. They studied in detail only the case where the dead layer thickness is much smaller than the film thickness. For this case,  $d_c$  proved to be independent of the ferroelectric slab thickness but depended on ferroelectric material constants and the dielectric constant of the paraelectric layer.<sup>21</sup> We are interested in the case where the two thicknesses are comparable. Nevertheless, some general formulae of ChT are relevant to our case also, and the phenomena in the cases of thin and thick dead layers for similar systems prove to be qualitatively similar. That is why it makes sense to discuss some of the ChT results and describe their procedure to some extent.

Note that for  $d > d_c$  where the phase transition is into a multidomain state, they found that two types of domain structures appear. If  $d - d_c < d_c$ , the period of the domain structure is larger than the thickness of the ferroelectric slab (“wide

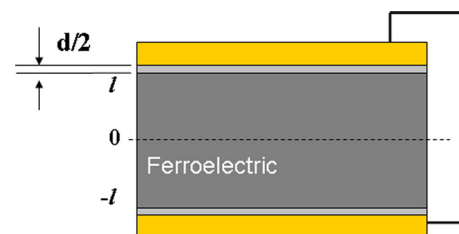


FIG. 1. (Color online) Schematic of the ferroelectric layer with thin dead layers having thickness  $d/2$  between the ferroelectric and the electrode. This was the system that was investigated in Ref. 18.

domains,” WD); for  $d - d_c > d_c$ , this period is less than the thickness (“narrow domains,” ND). In Ref. 19, these two regimes were called “strong coupling” and “weak coupling” regimes. In this work, we will show that in the case of sufficiently large dielectric constant of the paraelectric layer, one has to distinguish between the two different ND regimes.

To find the phase transition temperature, ChT studied stability of the paraelectric phase. The mathematical indication of a loss of stability of a state (phase) was obtained by studying solutions of an appropriate system of linear differential equations along with relevant boundary conditions. This method dates back to a paper by Suhl,<sup>22</sup> who used it in another problem. The paraelectric phase is stable when the only possible solution is zero (trivial). Appearance of non-zero (non-trivial) solutions indicates a way of loss of stability of the phase, and specifically this loss is with respect to a form of the ferroelectric polarization distribution that is represented by the solution. Within this approach, such a formulation of the problem results in infinite number of ways of stability loss represented by an infinite set of the polarization profiles. Of course, they are not real and are virtual possibilities of the stability loss. The loss of stability of the paraelectric phase, corresponding to the theoretically found phase transition, occurs with respect to a single form chosen from these infinite number of virtual solutions. The criterion of the choice is that the loss of stability of the paraelectric phase with respect to this solution occurs earliest, i.e., it corresponds to the highest temperature.

Similar to ChT we shall suppose that both the ferroelectric and paraelectric layers are isotropic in the  $x$ - $y$  plane. Then the nontrivial inhomogeneous solutions at the stability loss appear simultaneously for all the directions in this plane. That is why it is sufficient to consider inhomogeneities along one direction only, which we identify as the  $x$  axis. Thus the problem is reduced to solving the equations in the  $x$ - $z$  plane. The system of linear differential equations mentioned here includes the linearized constituent equation for the ferroelectric polarization ( $P_z$ )

$$AP_z - g \frac{\partial^2 P_z}{\partial x^2} - \eta \frac{\partial^2 P_z}{\partial z^2} = E_z, \quad (1)$$

where  $E_z$  is the electric field along  $z$  axis. Other equations should also be included to account for an (indirect) influence of  $P_z$  on other degrees of freedom. The most important of them is the polarization along  $x$  (nonferroelectric) axis. Because  $E_z(x)$  implies the presence of  $E_x$  via the electrostatic equation  $\text{curl} \mathbf{E} = 0$ , one has to take into account the  $E_x$  component together with the polarization, which we shall implicitly include by introducing the dielectric constant  $\varepsilon_\perp$  along the plane of the structure. The electric field due to the ferroelectric polarization exists, of course, also in the paraelectric, which we consider as isotropic with the dielectric constant  $\varepsilon_p$ . The system of equations become complete by adding  $\text{div} \mathbf{D} = 0$ , where  $\mathbf{D} = \varepsilon_0 \varepsilon_p \mathbf{E}$  in the paraelectric and  $\mathbf{D} = (\varepsilon_0 \varepsilon_\perp E_x, 0, \varepsilon_0 \varepsilon_b E_z + P_z)$  in the ferroelectric layer. In the latter formula, we have introduced the so-called “base” or “background” dielectric constant,  $\varepsilon_b$ , which is assumed to reflect the fact that  $P_z$  is not the total  $z$  component of the

polarization but is only the “soft part,” which corresponds to the order parameter.<sup>23</sup> In this way, we take into account more non-ferroelectric degrees of freedom.

Because we are considering an infinite slab, we can present the  $x$  dependence of all the functions in form of a Fourier series:  $P_z(x, z) = \sum_k P_{zk}(z) \cos kx$  and  $\varphi(x, z) = \sum_k \varphi_k(z) \cos kx$  to allow the system of the partial differential equations to be reduced to systems of ordinary differential equations. We work with the electrostatic potential  $\varphi(x, z)$  as it is convenient to use this instead of the electric field. In addition, following ChT, we put  $\eta = 0$  in Eq. (1); this considerably simplifies the mathematics and makes it possible to take into account the electrostatic boundary conditions only, which we have already commented on in Sec. I. Inserting the Fourier form of the polarization and the electrostatic potential into Eq. (1), we obtain an algebraic equation:

$$(A + gk^2)P_{zk} = -\frac{d\varphi_k}{dz} \quad (2)$$

and for a given  $k$  the electrostatic equation  $\text{div} \mathbf{D} = 0$  acquires now the form

$$\varepsilon_k \frac{d^2 \varphi_{fk}}{dz^2} - \varepsilon_\perp k^2 \varphi_{fk} = 0, \quad (3)$$

where

$$\varepsilon_k = \varepsilon_b + 1/\varepsilon_0(A + gk^2) \quad (4)$$

for the ferroelectric and subscript  $f$  implies the ferroelectric layer. For the paraelectric layer, we have

$$\frac{d^2 \varphi_{pk}}{dz^2} - k^2 \varphi_{pk} = 0 \quad (5)$$

where  $p$  implies the paraelectric layer.

Because of the symmetry of the system, we establish that there are two families of solutions: symmetric and anti-symmetric with respect to reflection in the mirror plane at  $z = 0$ . ChT considered antisymmetric solutions only guided by physical arguments. We shall consider both families of solutions to illustrate our treatment of larger systems where these two solutions can, in principle, compete in terms of the earlier stability loss. In both cases, one can use the boundary conditions at two of the four interfaces, e.g., at  $z = l/2$  and  $z = (l + d)/2$ :

$$\varphi_k((l + d)/2) = 0, \quad (6)$$

$$\varphi_k(l/2 + 0) = \varphi_k(l/2 - 0), \quad (7)$$

$$\varepsilon_k \frac{d\varphi_k}{dz}(l/2 - 0) = \varepsilon_p \frac{d\varphi_k}{dz}(l/2 + 0). \quad (8)$$

One can show that for  $\varepsilon_k > 0$  no nontrivial solution of either family is possible, i.e., the nonpolar phase is stable. For  $\varepsilon_k < 0$ , we begin with the antisymmetrical case looking for solutions in the form  $\varphi_{fk}(z) = C \sin qz$ , where

$$q = k \sqrt{\varepsilon_\perp / |\varepsilon_k|} \quad (9)$$

for the ferroelectric and  $\varphi_{pk}(z) = F \sinh k(z - (l+d)/2)$  for the paraelectric. Equations (7) and (8) attain the form

$$C \sin ql/2 + F \sinh kd/2 = 0, \quad (10a)$$

$$C \varepsilon_k q \cos ql/2 - F \varepsilon_p k \cosh kd/2 = 0. \quad (10b)$$

Non-trivial solutions for Equations (10a) and (10b) exist if

$$\tan ql/2 = \left( \sqrt{|\varepsilon_k| \varepsilon_{\perp}} / \varepsilon_p \right) \tanh kd/2. \quad (11)$$

In the limit of  $d \rightarrow \infty$ , this formula becomes

$$\tan ql/2 = \sqrt{|\varepsilon_k| \varepsilon_{\perp}} / \varepsilon_p, \quad (12)$$

which is relevant to phase transition into multidomain state in a non-electroded slab in an infinite medium with the dielectric constant  $\varepsilon_p$ . We shall repeatedly revisit this formula throughout this paper.

For the symmetrical case instead of Eq. (11), we start from  $\varphi_{pk}(z) = C \cos qz$ . Then instead of Eqs. (10a) and (10b), we have

$$C \cos ql/2 + F \sinh kd/2 = 0, \quad (13a)$$

$$C \varepsilon_k q \sin ql/2 + F \varepsilon_p k \cosh kd/2 = 0, \quad (13b)$$

from where the condition of nontrivial solution is obtained as

$$\tan ql/2 = - \left( \varepsilon_p / \sqrt{|\varepsilon_k| \varepsilon_{\perp}} \right) \coth kd/2. \quad (14)$$

Because the rhs (right hand side) of this equation is negative, the argument of the tangent should be more than  $\pi/2$  unlike to Eq. (11). Therefore, for the same value of  $k$ , the value of  $q$  of the symmetric family is larger than of the antisymmetric family, i.e.,  $|\varepsilon_k|$  is less in the symmetric case than in the antisymmetric one. From Eq. (4), one sees that this corresponds to larger  $|A|$ , i.e., to a lower temperature of the stability loss than for the solution with the same  $k$  of the antisymmetric family. Physically, this is quite natural: A symmetric potential in the ferroelectric layer means that both the electric field and the ferroelectric polarization [see Eq. (4)] are zero at the central plane of the slab, and this is energetically less profitable than to have the polarization of the same sign for all the values of  $z$ . Therefore, one has to discuss Eq. (11) to find the function  $A_{ls}(k)$ , which defines the limit of stability of the nonpolar phase with respect to the appearance of the ‘‘polarization wave’’ with a given  $k$ . As we have already mentioned, to find the real limit of the stability, one has to find the ‘‘weakest point,’’ i.e., the value of  $k$  that corresponds to the maximum value of  $A_{ls}(k)$  where the ‘‘first’’ stability loss corresponding to the highest temperature occurs.

## B. The Chensky-Tarassenko cell with thick dead layer

It is easy to find the function  $A_{ls}(k)$  for small  $k$  and large  $k$  regions. ChT found it for the case of very thin dead layer, but it is just as straightforward not to make this assumption and consider dead or paraelectric layers of thickness comparable to that of the ferroelectric. The cell studied in this

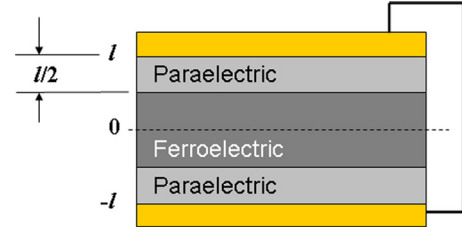


FIG. 2. (Color online) ChT cell with thick dead layers where each paraelectric layer is  $l/2$ .

section is displayed in Fig. 2. To avoid overloading the paper with formulae, we shall not consider the general case but only that of  $d = l$ , i.e., we have:

$$\tan ql/2 = \left( \sqrt{|\varepsilon_k| \varepsilon_{\perp}} / \varepsilon_p \right) \tanh kl/2. \quad (15)$$

For the small  $k$  region, one can expand both sides of Eq. (15) in terms of  $k$  and  $q$  taking first into account the first two terms only:

$$\sqrt{\frac{1}{|\varepsilon_k| \varepsilon_{ls}}} \left( 1 + \frac{\varepsilon_{\perp} k^2 l^2}{12 |\varepsilon_k| \varepsilon_{ls}} \right) = \frac{\sqrt{|\varepsilon_k| \varepsilon_{\perp}}}{\varepsilon_p} \left( 1 - \frac{k^2 l^2}{12} \right). \quad (16)$$

Putting in this equation  $k = 0$  and also differentiating it with respect to  $k^2$  and then putting  $k = 0$ , we find two first terms in the Taylor expansion for  $|\varepsilon_k| \varepsilon_{ls}$  in terms of  $k^2$ .

$$|\varepsilon_k| \varepsilon_{ls} = \varepsilon_p + \frac{k^2 l^2 (\varepsilon_p + \varepsilon_{\perp})}{12}. \quad (17)$$

Using Eq. (4), one obtains

$$A_{ls} = - \frac{1}{\varepsilon_0 (\varepsilon_b + \varepsilon_p)} + \left( \frac{l^2 (\varepsilon_p + \varepsilon_{\perp})}{12 \varepsilon_0 (\varepsilon_b + \varepsilon_p)^2} - g \right) k^2 + \dots \quad (18)$$

The first term corresponds to the loss of stability with respect to a single domain state. Depending on the sign of the coefficient at  $k^2$ , the loss of stability with respect to a ‘‘polarization wave’’ with  $k \neq 0$  corresponds to larger or smaller values of  $A$ , i.e., to an ‘‘earlier’’ or to a ‘‘later’’ event. Because the ‘‘later’’ stability loss is of no interest, the phase transition is into a multidomain state if the coefficient is positive and is to a single domain state if the coefficient is negative. Zero value of the coefficient at  $k^2$  in Eq. (18) defines the ‘‘critical’’ value of  $l$  ( $l_c$ ), which separates the phase transitions into single and multi-domain states. For  $l < l_c$ , the function  $A_{ls}(k)$  has maximum at  $k = 0$ . One can thus see that

$$l_c^2 = 12 \varepsilon_0 g (\varepsilon_b + \varepsilon_p)^2 / (\varepsilon_p + \varepsilon_{\perp}) \simeq 12 \varepsilon_0 g \varepsilon_p^2 / (\varepsilon_p + \varepsilon_{\perp}), \quad (19)$$

where we have supposed that  $\varepsilon_p \gg \varepsilon_b$ , which is usually the case for systems of experimental interest. We shall restrict ourselves to this case only. Because  $\varepsilon_0 g \simeq 1 \text{ \AA}^2$  (see, e.g., Ref. 24) for the case  $\varepsilon_{\perp} \gg \varepsilon_p$  one finds from Eq. (19) that  $l_c$  is less than unit cell distance, meaning no phase transition into single domain state is possible. If, on the contrary,  $\varepsilon_p > \varepsilon_{\perp}$ , which is what one has for  $\text{BaTiO}_3\text{-SrTiO}_3$  superstructure, the  $l_c$  can be considerably larger than the unit cell

distance and our use of a continuous medium theory to consider interplay between single- and multidomain formation at the phase transition is quite consistent and valid. We shall keep our focus on this case.

Proceeding further with the analysis of Eq. (15), we begin focus on the small  $k$  (WD) region by finding the next,  $k^4$ , term in Eq. (18). One has to take into account the next terms in expansions of the tan and tanh in Eq. (15) to obtain:

$$\begin{aligned} & \sqrt{\frac{1}{|\varepsilon_k|_{ls}}} \left( 1 + \frac{\varepsilon_{\perp} k^2 l^2}{12 |\varepsilon_k|_{ls}} + \frac{\varepsilon_{\perp}^2 k^4 l^4}{120 |\varepsilon_k|_{ls}^2} \right) \\ &= \frac{\sqrt{|\varepsilon_k|_{ls}}}{\varepsilon_p} \left( 1 - \frac{k^2 l^2}{12} + \frac{k^4 l^4}{120} \right). \end{aligned} \quad (20)$$

In addition to the preceding operations, we differentiate this equation with respect to  $k^2$  two times and put  $k=0$  to find

$$|\varepsilon_k|_{ls} = \varepsilon_p + k^2 l^2 (\varepsilon_p + \varepsilon_{\perp}) / 12 + k^4 l^4 (\varepsilon_{\perp}^2 - \varepsilon_p^2) / (720 \varepsilon_p), \quad (21)$$

$$\begin{aligned} \varepsilon_0 A_{ls} = & -\frac{1}{\varepsilon_p} + \frac{(l^2 - l_c^2)(\varepsilon_p + \varepsilon_{\perp})}{12 \varepsilon_p^2} k^2 \\ & - \frac{(\varepsilon_{\perp} + \varepsilon_p)(3\varepsilon_p + 2\varepsilon_{\perp}) k^4 l^4}{360 \varepsilon_p^3}. \end{aligned} \quad (22)$$

For  $l > l_c$ , the value of  $k$  corresponding to the maximum of function  $A_{ls}(k)$  and, therefore, to the phase transition is

$$k^2 = k_c^2 = \frac{15(l^2 - l_c^2)(\varepsilon_p + \varepsilon_{\perp})}{l^4(3\varepsilon_p + 2\varepsilon_{\perp})} \simeq \frac{5(l^2 - l_c^2)}{l^4}, \quad (23)$$

where once more we have assumed that  $\varepsilon_p > \varepsilon_{\perp}$ . We see from this formula that the WD regime ( $kl < 1$ ) is possible only at, approximately,

$$l - l_c < l_c/3, \quad (24)$$

i.e., the range of  $l$  corresponding to WD is fairly small. The phase transition temperature is determined by

$$\varepsilon_0 A_{ls}(k_c) = -\frac{1}{\varepsilon_p} \left( 1 - \frac{5(l - l_c)^2 (\varepsilon_p + \varepsilon_{\perp})}{2l_c^2 (3\varepsilon_p + 2\varepsilon_{\perp})} \right), \quad (25)$$

where Eq. (24) is taken into account. Before making sure that Eq. (25) is valid in the region defined by Eq. (24), we have to check if the condition related to the possibility to expand the tan function in Eq. (15), i.e.,  $ql < 1$ , is also satisfied. One sees from Eq. (25) that at the boundary of the WD regime, i.e., at  $l - l_c \simeq l_c/3$ , the value of  $A_{ls}(k_c)$  is nearly the same as for  $l = l_c$ , meaning  $|\varepsilon_k|_{ls} \simeq \varepsilon_p$ . Taking into account Eq. (9), we see that at the boundary of the WD regime  $qc_l \simeq \sqrt{\varepsilon_{\perp}/\varepsilon_p} \ll 1$ .

The preceding finding would also mean that if  $\varepsilon_p \gg \varepsilon_{\perp}$  there exists a narrow domain (ND) regime ( $kl > 1$ ) with small changes of the values (electric field, polarization) across the ferroelectric layer ( $ql < 1$ ). We shall call it the NDS regime. Because within this regime  $qc_l < 1$  while  $k_c l > 1$ , Eq. (15) can be approximated as

$$ql/2 = \sqrt{|\varepsilon_k|_{ls}} / \varepsilon_p \quad (26)$$

or

$$|\varepsilon_k| = \varepsilon_p kl/2. \quad (27)$$

Using Eq. (4) one then obtains

$$A_{ls}(k) = -2(\varepsilon_0 \varepsilon_p kl)^{-1} - gk^2. \quad (28)$$

The maximum of this function corresponds to

$$k = k_c = (\varepsilon_0 \varepsilon_p gl)^{-1/3}, \quad (29)$$

and the expected phase transition temperature is defined by

$$\begin{aligned} A_{ls}(k_c) = & -2(\varepsilon_0 \varepsilon_p gl)^{1/3} (\varepsilon_0 \varepsilon_p l)^{-1} - g(\varepsilon_0 \varepsilon_p gl)^{-2/3} \\ = & -3g^{1/3} (\varepsilon_0 \varepsilon_p)^{-2/3} l^{-2/3}. \end{aligned} \quad (30)$$

The NDS regime, which evidently begins at  $l \simeq (1.5 - 2)l_c$ , ends when  $qc_l$  approaches unity. Using Eqs. (26), (27), and (29), one finds that this happens around

$$l \simeq l_{\sim} = (\varepsilon_p / \varepsilon_{\perp})^{3/2} l_c. \quad (31)$$

One sees that if  $\varepsilon_p \gg \varepsilon_{\perp}$ , the NDS regime corresponds to a broad interval of  $l$ .

At  $l > l_{\sim}$ , one has  $\tan ql/2 \gg 1$  (NDL regime with large change of values across the thickness of the layer) or

$$q \simeq \pi/l, \quad (32)$$

i.e., this is the case well studied by ChT, who showed (see also Ref. 19) that for the phase transition and the period of the sinusoidal domain structure one has:

$$A_{ls}(k_c) = -2\pi g^{1/2} (\varepsilon_0 \varepsilon_{\perp})^{-1/2} l^{-1} \quad (33)$$

$$k_c^2 = \pi (\varepsilon_0 \varepsilon_{\perp} g)^{-1/2} l^{-1}. \quad (34)$$

We see that here the phase transition point as well as the period of the domain structure does not depend on  $\varepsilon_p$ . We illustrate the results in Fig. 3 using Eq. (22) for the small  $l$  regime and Eq. (30) for the large  $l$  regime in comparison with the numerical solution of Eq. (15) for a maximum  $l$  of 20 nm.

### C. Bilayer

Figure 4 illustrates the system we now want to discuss. It is straightforward to do so within the ChT approach summarized in the previous subsection. The solutions for  $\varphi_k(z)$  are now  $\varphi_k(z) = C \sin qz$  for the ferroelectric layer and  $\varphi_k(z) = F \sinh k(z - 2l)$  for the paraelectric one. The boundary conditions at  $z = l$  are:

$$C \sin ql + F \sinh kl = 0, \quad (35)$$

$$C \varepsilon_k q \cos ql - F \varepsilon_p k \cosh kl = 0. \quad (36)$$

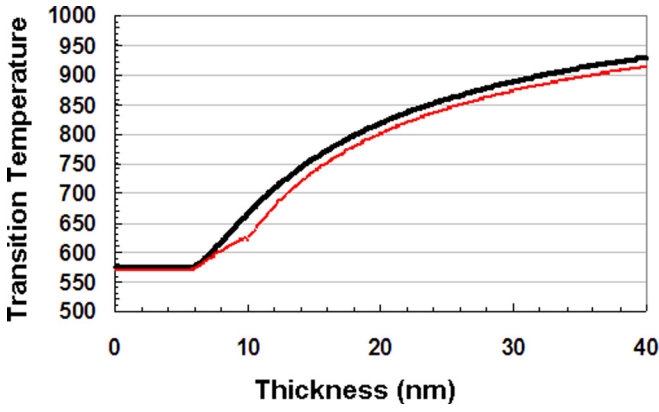


FIG. 3. (Color online) Comparison between the analytical (thin line) and the numerical (thick line) results of the transition temperature (in °C) in the ChT cell for  $\epsilon_p = 500$ . The thin curve reflect the small  $kl$  and the large  $kl$  limits as given in Eqs. (22) and (30). The material parameter values used in the calculations are  $T_c = 998^\circ\text{C}$ , Curie constant  $= 1.5 \times 10^5$ ,  $g = 6.2 \times 10^{-10} \text{ m}^3/\text{F}$ ,  $\epsilon_\perp = 50$ .

Comparing this with Eqs. (10a) and (10b) for  $d = l$ , we see that one has to substitute  $l$  for  $2l$  in this equation to obtain Eqs. (35) and (36) so that instead of Eq. (15) one has:

$$\tan ql = \left( \sqrt{|\epsilon_k| \epsilon_\perp} / \epsilon_p \right) \tanh kl. \quad (37)$$

In the same way, all the results from the previous subsection can be transformed into the results for the bilayer. In particular, one sees that the critical value of  $l$  separating the single domain, and the wide domain regimes is now two times less than in the previous case. Furthermore, for very large  $ls$ , the difference between the phase transition temperature and the Curie temperature  $T_c$  ( $A(T_c) = 0$ ) is two times smaller in the case of the bilayer than in the ChT case of a symmetrical trilayer. The transition temperatures and  $k_c$  as a function of layer thickness for three different values of  $\epsilon_p$  are given in Fig. 5.

**D. Non-symmetrical trilayer**

Without any algebra, one can expect the value of  $l_c$  to be larger than for the bilayer and smaller than for the symmetrical trilayer. The system and the notations are presented in Fig. 6. We write the solutions for the potential in the form:

$$\varphi_k(z) = F_1 \sinh kz \quad (38)$$

for  $0 < z < l_1$

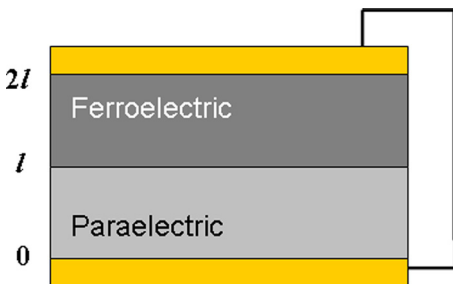


FIG. 4. (Color online) Bilayer cell with ferroelectric and paraelectric layers of equal thickness.

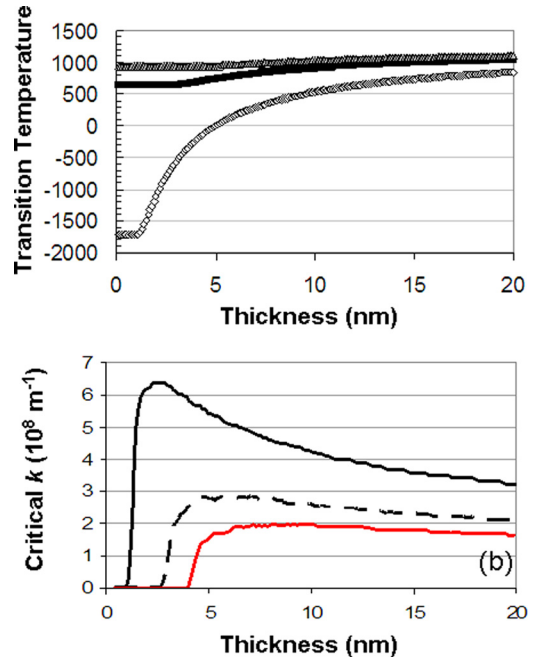


FIG. 5. (Color online) (a) Transition temperatures (in °C) as a function of layer thickness for the bilayer cell for  $\epsilon_p = 100$  (hollow diamonds),  $\epsilon_p = 500$  (dark thick line), and  $\epsilon_p = 1000$  (gray triangles) and (b) Critical  $k$  as a function of layer thickness for the bilayer cell  $\epsilon_p = 100$  (solid line),  $\epsilon_p = 500$  (dashed line), and  $\epsilon_p = 1000$  (line with the smallest  $k$  values). The material parameter values used in the calculations are  $T_c = 998^\circ\text{C}$ , Curie constant  $= 1.5 \times 10^5$ ,  $g = 6.2 \times 10^{-10} \text{ m}^3/\text{F}$  and  $\epsilon_\perp = 50$ .

$$\varphi_k(z) = C \sin q(z - l_1) + D \cos q(z - l_1) \quad (39)$$

for  $l_1 < z < l_1 + l$  and

$$\varphi_k(z) = F_2 \sinh k(z - 2l) \quad (40)$$

for  $l_1 + l < z < 2l$ . The boundary conditions at  $z = l_1$  read:

$$C \sinh kl_1 = D, \quad (41)$$

$$\epsilon_p k F_1 \cosh kl_1 = -|\epsilon_k| q C \quad (42)$$

and at  $z = l_1 + l$ :

$$C \sin ql + D \cos ql = -F_2 \sinh k(l - l_1), \quad (43)$$

$$-|\epsilon_k| q (C \cos ql - D \sin ql) = \epsilon_p k F_2 \cosh k(l - l_1). \quad (44)$$

With the help of Eqs. (41) and (42), it is easy to reduce the system to two equations only:

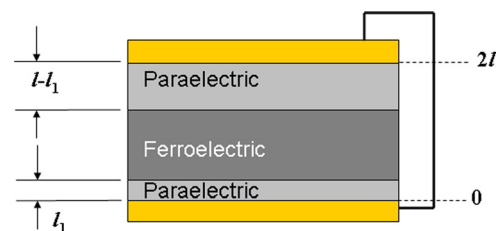


FIG. 6. (Color online) Schematic of the non-symmetrical trilayer.

$$F_1(|\varepsilon_k|q \sinh kl_1 \cos ql - \varepsilon_p k \cosh kl_1 \sin ql) + F_2|\varepsilon_k|q \sinh k(l-l_1) = 0, \quad (45)$$

$$C(\varepsilon_p k \cosh kl_1 \cos ql + |\varepsilon_k|q \sinh kl_1 \sin ql) - F_2 \varepsilon_p k \cosh k(l-l_1) = 0. \quad (46)$$

The condition of existence of non-trivial solutions of this system reads

$$\left[ (\varepsilon_p k)^2 - |\varepsilon_k|^2 q^2 \tanh kl_1 \tanh k(l-l_1) \right] \tan ql = |\varepsilon_k|q k \varepsilon_p [\tanh k(l-l_1) + \tanh kl_1]. \quad (47)$$

To be specific, we shall assume that  $l_1 < l/2$ , i.e.,  $l-l_1 > l/2$ . For large  $ls$ , we expect that  $kl_1 \gg 1$  then also  $k(l-l_1) \gg 1$ . In this case, both  $\tanh kl_1$  and  $\tanh k(l-l_1) \simeq 1$ , and Eq. (47) acquires the form

$$\tan ql = \frac{2|\varepsilon_k|q k \varepsilon_p}{(\varepsilon_p k)^2 - a^2 q^2}$$

or

$$\tan ql/2 = \frac{|\varepsilon_k|q}{\varepsilon_p k} = \frac{\sqrt{|\varepsilon_k|\varepsilon_\perp}}{\varepsilon_p},$$

which coincides with Eq. (12).

We see that for sufficiently large  $ls$ , the system “forgets” the absence of symmetry. For small  $l$ , the situation is, however, different. Let us find  $l_c$  for this case. To realize this aim, one has to expand  $\tanh$  and  $\tan$  functions in Eq. (47) keeping the first two terms only. As a result one finds that

$$|\varepsilon_k| = \varepsilon_p \left( 1 + \frac{(\varepsilon_\perp + \varepsilon_p)k^2}{3\varepsilon_p} (l^2 - 3l_1(l-l_1)) \right) \quad (48)$$

$$A_{ls}(k) = -\frac{1}{\varepsilon_0(\varepsilon_b + \varepsilon_p)} + \left( \frac{(\varepsilon_\perp + \varepsilon_p)}{3\varepsilon_0(\varepsilon_b + \varepsilon_p)^2} l^2 \left( 1 - 3\frac{l_1(l-l_1)}{l^2} \right) - g \right) k^2, \quad (49)$$

i.e., in this case

$$l_c^2 = \frac{3g\varepsilon_0(\varepsilon_b + \varepsilon_p)^2}{(\varepsilon_\perp + \varepsilon_p) \left( 1 - 3\frac{l_1(l-l_1)}{l^2} \right)}. \quad (50)$$

We see that at  $l_1 = l/2$  Eq. (50) coincides with Eq. (19), whereas at  $l_1 = 0$ , it provides  $l_c$ , which is half of the previous one. Figure 7 illustrates the dependencies of the phase transition temperature and of  $k_c$  on  $l$  for all the cases (ChT cell, bilayer cell and non-symmetrical trilayer) considered in the preceding text. Note that in all three cases, the transition temperature into the single domain state is the same.

### III. LARGE SYSTEMS

We would now like to discuss systems with many layers. The schematics of the two systems are given in Fig. 8. The

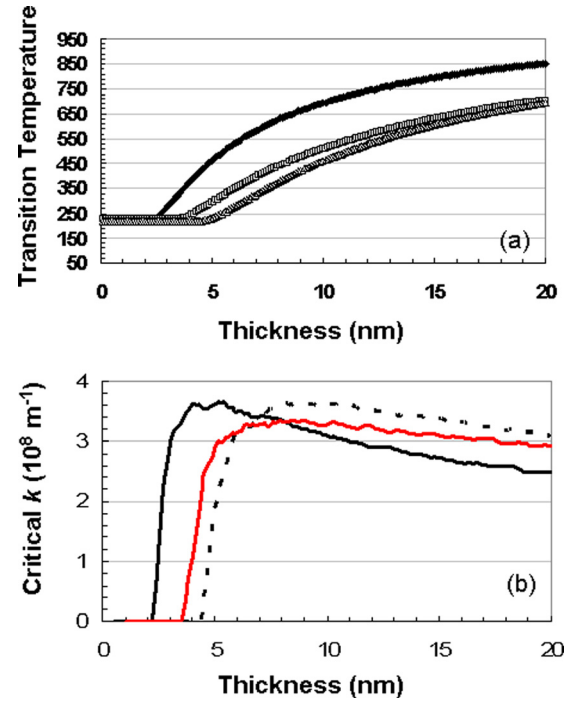


FIG. 7. (Color online) Comparison of (a) the numerical solutions for transition temperature for the bilayer cell (solid thick line), the non-symmetrical cell with  $l/4$ ,  $3l/4$  paraelectric layer partitioning (hollow squares) and the ChT cell (hollow triangles); (b) the  $k_c$  at the transition for the bilayer cell (thick solid line), the asymmetrical cell (line starting at 3.7 nm along the thickness axis), and the ChT cell (dashed line) for the BaTiO<sub>3</sub>—SrTiO<sub>3</sub> system. The values used for BaTiO<sub>3</sub> fully strained on SrTiO<sub>3</sub> in the calculations are  $T_C = 998^\circ\text{C}$  (computed using the constants given in Ref. 25, Curie constant =  $1.5 \times 10^5$  °C,  $g = 6.2 \times 10^{-10}$  m<sup>3</sup>/F,  $\varepsilon_\perp = 20$ ,  $\varepsilon_p = 300$  for SrTiO<sub>3</sub> and, for the sake of convenience, is assumed to be constant over the entire temperature range.

assumption about periodicity made in Refs. 19 and 20, i.e., about irrelevance of conditions at the boundaries of a very large multilayer structure, can be questioned using simple physical arguments. Let us consider the virtual loss of stability of the paraelectric phase in a very large multilayer structure with respect to a single domain ferroelectric state assuming the periodicity along the thickness of the structure. The assumption of periodic boundary conditions is equivalent to considering the ChT cell as a small system with short-circuited electrodes. We have found out in the previous section that the loss of stability of the paraelectric state to single domain ferroelectric state occurs at

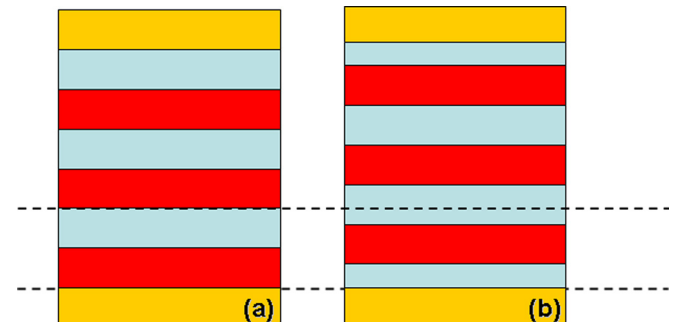


FIG. 8. (Color online) Schematic showing unit cells of the superstructure consisting of (a) bilayers and (b) ChT cells.

$$A_{ls}(0) = -\varepsilon_0^{-1}(\varepsilon_b + \varepsilon_p)^{-1} \quad (51)$$

(compare with Eqs. (18) and (49)). Let us show that this result is not necessarily correct. Whether Eq. (51) is correct or not depends on whether the multilayer system as whole is supplied by metallic electrodes and whether these electrodes are short-circuited. Imagine that there are no such electrodes. Then the condition  $dD_z/dz = 0$  inside the superstructure and  $\mathbf{D} = 0$  beyond the multilayer give us the result that  $\mathbf{D} = 0$  at every point of the multilayer (recall that we consider a possible single domain state, i.e., there are no dependencies along the  $x$  and  $y$  axes). As a result for a homogeneously polarized state

$$E_z = -P_z/(\varepsilon_b \varepsilon_0), \quad (52)$$

and from Eq. (1) it follows that

$$(A + \varepsilon_0^{-1} \varepsilon_b^{-1})P_z = 0, \quad (53)$$

meaning that the loss of stability of the paraelectric phase with respect to a single domain state occurs at

$$A_{ls} = -\varepsilon_0^{-1} \varepsilon_b^{-1}, \quad (54)$$

which differs very substantially from Eq. (51). In other words, the loss of stability of the paraelectric phase with respect to appearance of a single domain ferroelectric state depends on the conditions at the boundaries of the multilayer. Therefore the idea about an infinite multilayer cannot be applied to this problem. Physically, this is quite natural because both in this work and work of others,<sup>19,20</sup> one considers layers of infinite lateral sizes, i.e., the sizes of the external electrodes or of a non-electroded external surface are always larger than the full thickness of the multilayer system. Experimentally, the ratio of the lateral sizes and the thickness is never less than at least an order of magnitude. Therefore, no point inside the multilayer system is “far enough” from the surface. As to the transition into single domain state, we argue in Sec. IV that the case of complete absence of electrodes or any short circuiting is of a fairly academic nature and the periodic boundary conditions are acceptable almost irrespective of the presence or absence of electrodes. This is not however necessarily so for the phase transition into multidomain states.

To understand the basis of the latter statement, let us consider a system of two bilayers (Fig. 9). One sees that the conditions for screening of the stray electric field arising when a domain structure is formed in the layer are different for layers 1 and 2. For the layer 1, a stray field exists



FIG. 9. (Color online) Two bilayer cell system mentioned in Sec. III A.

mainly near one interface (ferroelectric-paraelectric interface), whereas for the second layer, it exists near the two interfaces. It is thus evident that the polarization profile at the phase transition will be different in the two ferroelectric layers. It is worthwhile considering this case in more detail because the number of the ferroelectric-paraelectric interfaces is still relatively small, and the treatment of this case can be performed without too much algebra.

### A. Two bilayers

The solutions for  $\varphi_k(z)$  we shall write in the form  $\varphi_{f1k}(z) = C_1 \sin qz$  and  $\varphi_{f2k}(z) = C_2 \sin q(z-2l) + D_2 \cos q(z-2l)$  for the two ferroelectric layers and  $\varphi_{p1k}(z) = F_1 \sinh q(z-l) + G_1 \cosh q(z-l)$  and  $\varphi_{p2k}(z) = F_2 \sinh q(z-4l)$  for the two paraelectric layers. The short-circuited electrodes are taken into account in the first and in the last formulas.

It is convenient to introduce here dimensionless parameters:

$$\alpha = |\varepsilon_k|/\varepsilon_p, \quad \xi = \varepsilon_p/\varepsilon_{\perp}. \quad (55)$$

Note that the loss of stability with respect to homogeneous polarization corresponds to  $\alpha = 1$  and the values of  $\alpha$  of interest are larger than unity. From the boundary conditions at  $z = l$ , one finds

$$G_1 = C_1 \sin ql, \quad F_1 = -C_1 \sqrt{\alpha/\xi} \cos ql. \quad (56)$$

Next, from the boundary conditions at  $z = 2l$ , we find

$$\begin{aligned} C_2 &= C_1 \left( \cos ql \cosh kl - \sqrt{\xi/\alpha} \sin ql \sinh kl \right), \\ D_2 &= C_1 \left( -\sqrt{\alpha/\xi} \cos ql \sinh kl + \sin ql \cosh kl \right) \end{aligned} \quad (57)$$

and from the conditions at  $z = 3l$ , two formulas for  $F_2$  are

$$F_2 = C_1 \left[ \sqrt{\xi/\alpha} \sin^2 ql + \sqrt{\alpha/\xi} \cos^2 ql - \sin 2ql \coth kl \right] \quad (58)$$

and

$$F_2 = C_1 \left[ 2^{-1} \sin 2ql \tanh kl (1 - \alpha/\xi) - \sqrt{\alpha/\xi} \cos 2ql \right]. \quad (59)$$

The equivalence of these formulas gives us the condition of the existence of non-trivial solutions, which can be written as a quadratic equation for  $\tan ql$

$$\begin{aligned} & \left( \sqrt{\xi/\alpha} - \sqrt{\alpha/\xi} \right) \tan^2 ql \\ & - [(1 - \alpha/\xi) \tanh kl + 2 \coth kl] \tan ql + 2\sqrt{\alpha/\xi} = 0, \end{aligned} \quad (60)$$

the solutions of which are

$$(\tan ql)_1 = \sqrt{\alpha/\xi} \tanh kl \quad (61a)$$

$$(\tan ql)_2 = \frac{2 \coth kl}{\sqrt{\xi/\alpha} - \sqrt{\alpha/\xi}}. \quad (61b)$$

Note that Eq. (61a) coincides with Eq. (37) for a bilayer, but before concluding that the phase transition temperature in the two-bilayer is the same as in a single-bilayer, one has to study the possible stability losses that follow from Eq. (61b) to figure out if these stability losses correspond to lower temperatures than those following from Eq. (61a). At  $\xi \gg 1$ , there is an interval for values of  $\alpha$ :  $1 < \alpha < \xi$ , which is both of interest ( $\alpha > 1$ ) and corresponds to the positive sign of the lhs of Eq. (61b). Because  $q = k\sqrt{1/\alpha\xi} < k$ , the solutions of Eq. (61b) are possible for  $kl > 1$ , and  $\coth kl$  can be replaced by unity. Equation (61b) then reads

$$ql = 2\sqrt{\alpha/\xi}, \quad (62)$$

which coincides with Eq. (26) discussed before. We have seen there that it is related to the loss of stability of the paraelectric phase in the ChT cell, which occurs at lower temperatures than in the bilayer system. This means that the solution given by Eq. (61b) is irrelevant to our studies. We shall discuss the physical reason for this irrelevance in the following text where we explain physically why Eq. (61b) corresponds to a “later” loss of stability compared to Eq. (61a).

It is worthwhile discussing the profile of the polarization arising at the phase transition. From Eqs. (57) and (61a) one sees that  $D_2 = 0$  and

$$C_2 = C_1 \cos ql / \cosh kl, \quad (63)$$

i.e., the polarization in the first and second ferroelectric layer is

$$P_{zf1} = C_1 |\varepsilon_k| \cos qz \cos kx, \quad (64a)$$

$$P_{zf2} = \frac{C_1 q \cos ql}{\cosh kl} |\varepsilon_k| \cos q(z-2l) \cos kx. \quad (64b)$$

Note that the amplitude of the “polarization wave” is smaller in the second ferroelectric layer than in the first one (Eq. (38)), as we expected from the beginning, and becomes exponentially small in the narrow domain regime. For the paraelectric layers, we have

$$\varphi_{p1} = -\frac{C_1 \sin ql}{\sinh kl} \sinh k(z-2l), \quad (65a)$$

$$\varphi_{p2} = -C_1 \frac{\cos ql \sin ql}{\cosh ql \sinh kl} \sinh k(z-4l). \quad (65b)$$

Note that although there is no electrode between the first paraelectric and the second ferroelectric layer ( $z = 2l$ ), the potential at this interface is zero.

Now we would like to find the polarization profile that corresponds to the second option given by Eq. (61b). We shall compare the amplitude of the “polarization wave” in the two ferroelectric layers. To this end, we should use Eq. (57) together with Eq. (61b). For the same conditions of the parameters that are necessary for existence of solution of Eq. (61b) ( $\alpha < \xi$ ,  $kl > 1$ ), we find for the polarization in the second ferroelectric layer

$$P_{zf2} = -C_1 q \cos ql \cosh kl |\varepsilon_k| \cos \left[ q(z-2l) - 2(\alpha/\xi)^{3/2} \right]. \quad (66)$$

We see that for this option the ferroelectric polarization in the second layer is larger than in the first one (it is also in the opposite direction). So it is quite natural that this latter option is less profitable for the system and corresponds to a loss of stability at a lower temperature.

## B. Many bilayers

The calculations for a three-bilayer system are already cumbersome. Instead of Eq. (60), one obtains a third-order equation for  $\tan ql$  with coefficients given by inconvenient formulae. Although one of the three solutions is still given by Eq. (61a), to analyze the stability loss corresponding to two other possible families (in the case that the third order equation has three real roots) seems to be beyond the present work. Considering more bilayers presents an even more prohibitive analysis. What we can easily show is that Eq. (61a) applies to systems with any number of bilayers. It is tempting to conclude from this fact that the phase transition temperature is the same for a short-circuited multilayer system consisting of any number of bilayers. This seems physically reasonable, but, unfortunately, we cannot show this mathematically because to do so we are obliged to study loss of stability with respect to solutions corresponding to all the families of solutions and the number of the families seem to increase concurrently with the number of ferroelectric layers in the system. We have seen for the case of the two-bilayer system that the second family cannot compete with the first one corresponding to Eq. (61a). But we see no easy way to show this for any number of the bilayers when the number of the families could be equal or at least comparable with the number of the bilayers. Thus we can only propose physical arguments to elaborate on the earliest loss of stability. One must note that the phase transition temperature in a single bilayer system is higher than in what we called the ChT cell with the same total thickness of the ferroelectric and the paraelectric because the ferroelectric in the bilayer system is in a “better position” for forming a multidomain system than in the ChT one. This privilege of the first ferroelectric layer, which is in contact with the electrode, is conserved in a system with any number of the bilayers. It is therefore quite natural that the profile of the polarization amplitude of the “polarization wave” appearing at the phase transition is larger in the first layer than in other layers that have no direct contact with an electrode. This is precisely what is given by the solution of Eq. (61a) that we have seen for the case of a two-bilayer system. We think that this property of solutions such as Eq. (61a) is the reason that other solutions are irrelevant to the transition similar to the one given by Eq. (61b). This is also supported by the results of our numerical simulations as discussed in the following section.

Technically, to show that the option given by Eq. (61a) exists, we first make a conjecture about the form of the solutions that correspond to this option for a system with any number of bilayers, and then we show that for this form the

boundary conditions are satisfied if Eq. (61a) holds. The formulation of the conjecture is based on the consideration of three- and four-bilayer systems. With the assumption that Eq. (61a) holds for three- and four-bilayer systems, the problem related to these systems is drastically simplified, and we are able to satisfy the boundary conditions, rendering this assumption valid. As a result we have conjectured that for any number of bilayers, the solution is of the form

$$\varphi_{fn} = C_1 \frac{\cos^{n-1} ql}{\cosh^{n-1} kl} \sin q(z - 2(n-1)l) \quad (67)$$

for  $n$ th ferroelectric layer and

$$\varphi_{pn} = -C_1 \frac{\cos^{n-1} ql \sin ql}{\cosh^{n-1} kl \sinh kl} \sinh k(z - 2nl) \quad (68)$$

for  $n$ th paraelectric layer.

Now we have to check whether Eqs. (61a), (67), and (68) allow us to satisfy the boundary conditions at the two interfaces of the  $n$ th ferroelectric layer. To check the boundary conditions between the  $(n-1)$ -th paraelectric layer and the  $n$ th ferroelectric layer ( $z = 2(n-1)l$ ), we first note that

$$\varphi_{pn-1} = -C_1 \frac{\cos^{n-2} ql \sin ql}{\cosh^{n-2} kl \sinh kl} \sinh k(z - 2(n-1)l). \quad (69)$$

Comparing Eqs. (67) and (68), we see that the continuity of the potential is satisfied. The condition of continuity of the normal component of the dielectric displacement reads

$$\varepsilon_p k C_1 \frac{\sin ql}{\sinh kl} = a q C_1 \frac{\cos ql}{\cosh kl} \quad (70)$$

and is satisfied if Eq. (61a) holds.

At the interface between the  $n$ -ferroelectric layer and the  $n$ -th paraelectric layer ( $z = (2n-1)l$ ), the potential is non-zero, but it is the same at the ferroelectric and at the paraelectric sides. The condition of continuity of the normal component of the dielectric displacement now reads

$$a q C_1 \cos ql = \varepsilon_p k C_1 \frac{\sin ql}{\sinh kl} \cosh kl \quad (71)$$

and is once more satisfied if Eq. (61a) holds. Therefore, we have proved that Eq. (61a) provides the condition of existence of non-trivial solutions given by Eqs. (67) and (68) for a system consisting of any number of bilayers. Figure 10 presents dependence of the amplitude of the ‘‘polarization wave’’ in ferroelectric and paraelectric layers appearing at the loss of stability of the paraelectric phase computed using Eqs. (67) and (68).

### C. Two ChT cells

The system we consider in this subsection is presented in Fig. 11. We can use its symmetry with respect to the mirror plane at the middle of the central paraelectric layer to find the possible solutions. Apart from antisymmetric solutions of potential, which correspond to identical polarization profiles in the two ChT cells, it is possible to have symmetric

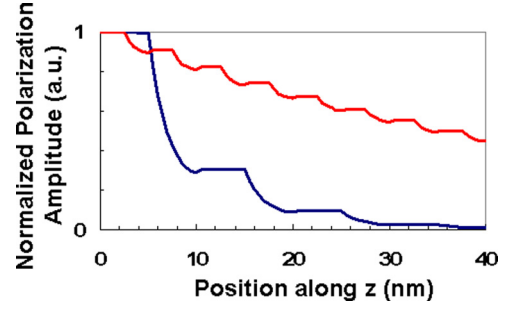


FIG. 10. (Color online) Polarization profile at the temperature of loss of stability of the paraelectric phase in the superstructure consisting of 4 bilayers (rapidly decaying curve from left to right with large period) and 8 bilayers (slowly decaying curve from left to right with small period) with 5 nm and 2.5 nm layer thickness, respectively. Note that the total thickness of the system in both cases is the same and fixed at 40 nm. The ferroelectric layers are BaTiO<sub>3</sub> and the paraelectric ones are SrTiO<sub>3</sub>. Critical thickness for single domain state stabilization is 2.2 nm. The 5 nm layer has a much more rapidly decaying polarization along the thickness. The values used for BaTiO<sub>3</sub> in the calculations are  $T_C = 998^\circ\text{C}$  (computed using the constants given in Ref. 25, Curie constant =  $1.5 \times 10^5^\circ\text{C}$ ,  $g = 6.2 \times 10^{-10} \text{ m}^3/\text{F}$ ,  $\varepsilon_{\perp} = 20$ ,  $\varepsilon_p = 300$  for SrTiO<sub>3</sub> and for the sake of convenience is assumed to be constant over the entire temperature range.

solutions. It is evident that the condition of existence of antisymmetric solutions is given by Eq. (15). Let us now find the condition for existence of symmetrical solutions. For the central paraelectric layer, such a solution can be only of type  $\varphi_{p2} = G_2 \cosh kz$  and for the third layer, it is  $\varphi_{p3} = F_3 \sinh k(z - 2l)$ . For the second ferroelectric layer, we shall take the solution in a general form:  $\varphi_{f2} = C_2 \sin qz + D_2 \cos qz$ , whereas for the first ferroelectric layer, it is to be found using the symmetry. From the boundary conditions at  $z = l/2$  one finds that

$$C_2 = G_2 \left( \sin ql/2 \cosh kl/2 - \sqrt{\xi/\alpha} \sinh kl/2 \cos ql/2 \right) \quad (72)$$

and

$$D_2 = G_2 \left( \cos ql/2 \cosh kl/2 + \sqrt{\xi/\alpha} \sin ql/2 \sinh kl/2 \right). \quad (73)$$

From the boundary conditions at  $z = 3l/2$ , we find

$$C_2 = -G_3 \left( \sin q3l/2 \sinh kl/2 + \sqrt{\xi/\alpha} \cosh kl/2 \cos q3l/2 \right) \quad (74)$$

and



FIG. 11. (Color online) Two ChT cell system mentioned in Sec. III C.

$$D_2 = -G_3 \left( \cos q3l/2 \sinh kl/2 - \sqrt{\xi/\alpha} \sin q3l/2 \cosh kl/2 \right). \quad (75)$$

Equating then the two formulae for  $C_2$  and  $D_2$ , we obtain a system of two equations for  $G_2$  and  $G_3$  and find the condition of existence of non-trivial solutions of this system. The latter turns out to be given by Eq. (61b), which we have already discussed considering two bilayers.

One should note that the importance of this family of solutions is, however, quite different. For large  $\xi$ , there is an interval of  $l$  where the two families of the solutions appear practically at the same temperature (see Fig. 12). Recall that a symmetrical solution means that the vectors of the ferroelectric polarizations are of opposite directions in the two ferroelectric layers. In a real, not exactly equilibrium situation, loss of stability may occur with respect to solutions of the two families, i.e., the profile of the polarization arising at the phase transition can consist of any linear combination of these solutions. Physically this is quite natural and corresponds to the situation that at large values of  $l$  the domain structures form practically independently in the two ferroelectric layers.

#### D. Many ChT cells

The same method that we applied to many bilayers can also be applied to a multilayer consisting of integer number of ChT cells the schematic of which is already given in Fig. 8(b). Here there are no “privileged” ferroelectric layers, and it is natural to expect that the profile of the polarization will be the same in all the ferroelectric (paraelectric) layers.

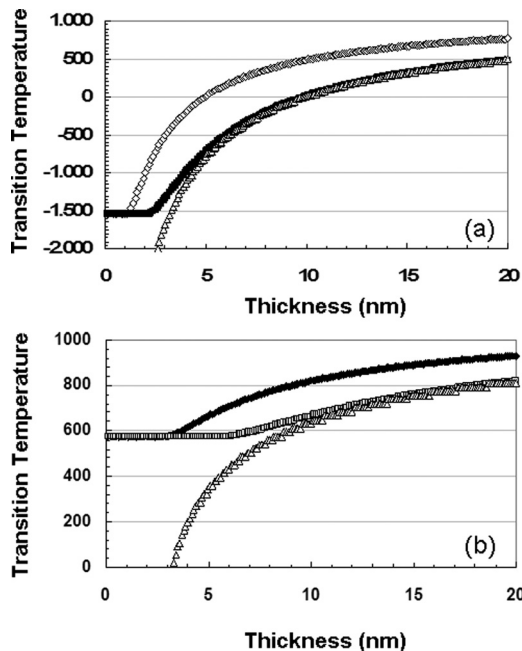


FIG. 12. Comparison of the transition temperatures (in °C) of the bilayer cell (solid line), the two-ChT cell (hollow squares) and the secondary solution (hollow triangles) of the two-bilayer and the two-ChT cell as a function of layer thickness for  $\epsilon_p = 100$  (a) and (b)  $\epsilon_p = 500$ . The material parameter values used in the calculations are  $T_C = 998^\circ\text{C}$ , Curie constant  $= 1.5 \times 10^5$  °C,  $g = 6.2 \times 10^{-10}$  m<sup>3</sup>/F,  $\epsilon_\perp = 50$ .

Starting from Eqs. (10a) and (10b), we can express the expected solution for this case as

$$\varphi_{fjk} = C \sin q \left( z - \frac{4n-3}{2} l \right), \quad (76a)$$

$$\varphi_{pjk} = C \frac{\sin ql/2}{\sinh kl/2} \sinh k \left( z - \frac{4n-1}{2} l \right). \quad (76b)$$

One can easily check that the both boundary conditions are satisfied at both interfaces ( $z = 2(n-1)l$  and  $z = (2n-1)l$ ) of  $n$ th ferroelectric layer if Eq. (15) holds. The polarization profile in the case of stability loss of the paraelectric phase to a multidomain polar state ( $l = 5$  nm and 8 nm) is given in Fig. 13.

#### IV. DISCUSSION

We have considered two types of superstructures consisting of either an arbitrary number of bilayers or what we have called ChT cells. The two superstructures are different only in the configuration of the layers neighboring the electrodes. In the bilayer case, namely the first superstructure, there is immediate contact between a ferroelectric layer and the ideal metallic electrode while the other electrode is in contact with a paraelectric layer. In the second case (second superstructure), both layers contacting the electrodes are paraelectric, having a thickness  $l/2$ . We have tried to calculate the ferroelectric phase transition temperature and to define the space distribution of ferroelectric polarization appearing at the phase transition when the electrodes are short-circuited. The method we have pursued is to study the possible ways of stability loss of the nonpolar phase and to identify the one that occurs first upon lowering the temperature. In this manner, one obtains both the phase transition temperature and the profile of the space distribution of the polarization just below the phase transition temperature.

The problem we attacked has proved to be too difficult to be rigorously solved because it became clear that, in general, in a large superstructure containing uniaxial ferroelectric layers with polar axis perpendicular to the layer plane,

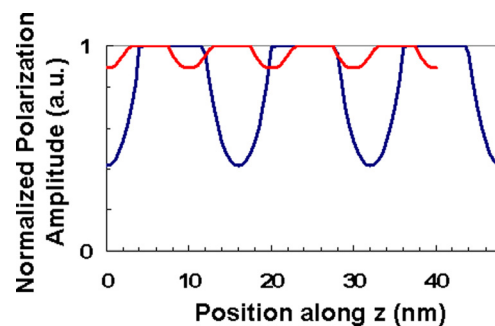


FIG. 13. (Color online) Polarization wave profile at the temperature of loss of stability of the paraelectric phase in the superstructure consisting of 3 ChT cells, each layer having 8 nm thickness (curve with large period), and 4 ChT cells with each layer being 5 nm thick (curve with small period). Critical thickness for single domain state stabilization is 4.4 nm. The values used for BaTiO<sub>3</sub> in the calculations are  $T_C = 998^\circ\text{C}$ , Curie constant  $= 1.5 \times 10^5$  °C,  $g = 6.2 \times 10^{-10}$  m<sup>3</sup>/F, and  $\epsilon_\perp = 20$ ,  $\epsilon_p = 300$  for SrTiO<sub>3</sub> and for the sake of convenience is assumed to be constant over the entire temperature range.

the ferroelectric polarization appearing at the phase transition is not periodic along the superstructure if the phase transition is into a multidomain state. This makes the number of different types of the polarization profiles with respect to which the nonpolar phase loses its stability comparable with the number of unit cells in a given superstructure. We were able to perform an exhaustive analysis of the loss of stability of the nonpolar phase only in the two smallest “superstructures” consisting of two bilayers or two ChT cells. We found two families of stability loss for every “small superstructure.” A comparison of these families of solutions is presented in Fig. 12. We have also shown that one of the solution families for both systems, specifically, those that correspond to the phase transitions in two-bilayer or in two-ChT cell systems is present in systems of any number of bilayers or ChT cells. We cannot prove mathematically that these families of the stability loss correspond to the phase transitions in very large superstructures as well, but we find this feasible physically and we assume this as a hypothesis. Therefore, when we mention “phase transition” in a superstructure we mean, strictly speaking, a hypothetical phase transition, which is also supported by our numerical simulations (see Fig. 14).

We found that if the dielectric constant of the paraelectric layer,  $\epsilon_p$ , is larger than  $\epsilon_{\perp}$ , there is an interval of  $l$ s for which the ferroelectric phase transition is into a single domain state. This interval goes from formally zero  $l$  (physically, of course, not less than unit cell distance) to some  $l$  that can be considerably larger than the unit cell size if  $\epsilon_p$  is sufficiently large. We focused our attention on this case, where our continuous medium approach is well justified. The maximum  $l$  that corresponds to the single domain regime we call  $l_c$ . Importantly, the value of  $l_c$  for the second superstructure ( $l_{c2}$ ) is two times that for the first one ( $l_{c2} = 2l_{c1}$ ). The physical reason for this is that in the first superstructure consisting of bilayers, the ferroelectric layer in immediate contact with the electrode is in a favorable position for formation of the domain structure: A part of the stray electric field associated with this structure is removed

by the electrode. This is why for  $l > l_{c1}$ , the phase transition temperature in the first superstructure is higher than in the second one with the same material parameters and period of the superstructure. The difference in the phase transition temperatures can be considerable. For the superstructure with the parameters of BaTiO<sub>3</sub> – SrTiO<sub>3</sub> system, this difference can be nearly 100 °C (see Fig. 7). Also note that the phase transition temperature in either superstructure does not depend on the number of unit cells comprising the superstructure and is the same as the phase transition temperature for a single bilayer or a single ChT cell.

Spectacularly, the polarization profile in the first superstructure (consisting of bilayers) is very different from that of the second superstructure (consisting of ChT cells) as shown in Figs. 10 and 13. We see that it is incorrect to assume periodicity along the out-of-plane direction of the superstructure if this is the superstructure consisting of what we call the bilayer cells. For the second superstructure, this is possible, but this superstructure is very specific because it is symmetric. The cause of the periodic nature of the profile is this symmetry not the large number of the unit cells in the superstructure. The first superstructure is not symmetric and this is also the case for any real superstructure. In Sec. II, we considered, as an example, a nonsymmetrical trilayer where the thickness of a paraelectric layer neighboring one of the electrodes is less than  $l/2$  and the other paraelectric layer neighboring the opposite electrode is thicker than  $l/2$  with the total thickness of these layers being  $l$ . We have seen that the maximum value of  $l$  corresponding to the phase transition into a single domain structure ( $l_{cn}$ ) falls between  $l_{c1}$  and  $l_{c2}$ . It proved to be algebraically too laborious to consider even a structure of two nonsymmetrical trilayers not to mention larger structures. It is of little doubt, however, that a superstructure the paraelectric layers of which contacting the electrodes with thickness different from  $l/2$  behaves qualitatively similarly to the first superstructure, i.e., the profile of the polarization arising at the phase transition is not periodic along the superstructure. To be fair, we should also mention that at sufficiently large  $l$  the lack of symmetry becomes

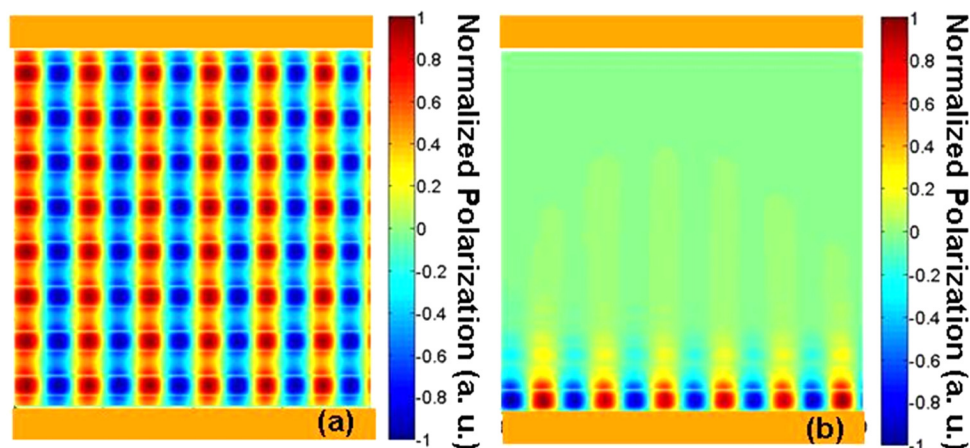


FIG. 14. (Color online) Polarization maps obtained in our numerical simulations 5 °C below the phase transition for the BaTiO<sub>3</sub>-SrTiO<sub>3</sub> system strained on a thick electroded SrTiO<sub>3</sub> substrate consisting of (a) 8 ChT cells and (b) 8 bilayers with each system having 80 nm total thickness. The system in (a) has a phase transition temperature around 300 °C and the one in (b) 440 °C, which agrees well with analytical results. The perpendicular colorbar scales are for normalized polarization. The values used for BaTiO<sub>3</sub> in the calculations are  $T_C = 998$  °C, Curie Constant =  $1.5 \times 10^5$  °C,  $g = 6.2 \times 10^{-10}$  m<sup>3</sup>/F,  $\epsilon_{\perp} = 20$ ,  $\epsilon_p = 300$  for SrTiO<sub>3</sub> and for the sake of convenience is assumed to be constant over the entire temperature range.

unimportant and the phase transition in a nonsymmetrical tri-layer is quite similar to that in the symmetrical ChT cell. This is quite natural and physically means that, at large  $l$ , formation of the domain structure in the ferroelectric layers proceeds similarly to what occurs in a ferroelectric layer in an infinite paraelectric medium. Clearly, the same phenomenon is expected in superstructures with large  $l$ s where the neighboring ferroelectric layers “do not feel each other” because intermediate paraelectric layers are too thick. Everything that we are discussing in this paper is of some real interest for superstructures with small  $l$ s. Here we mean the  $l$ s that are not very different from  $l_c$  for a given superstructure, which has to be calculated, of course, with a proper account of all its specific features. These features include the non-electrostatic effects at the interfaces and the configuration of the near electrode region. The latter is what is emphasized in this paper.

We should emphasize that the focus of our analysis in the preceding text is on multidomain phase transitions. For single domain states, however, the situation is quite different. As an example, consider a hypothetical single domain transition in a system with real electrodes. A real electrode can be modeled as an ideal metallic one with a dielectric “dead layer” at its surface (see, e.g., Ref. 24). It is easy to show that these parameters of the electrode do not influence the phase transition temperature and its other characteristics. Indeed, consider the superstructure presented in Fig. 15. Because the electric displacement is the same through the superstructure, one can see that the electric field is the same ( $E_f$ ) in all the ferroelectric layers and it is also the same ( $E_p$ ) in all the paraelectric ones. Therefore we have

$$-|\varepsilon_f|E_f = \varepsilon_p E_p = \varepsilon_e E_d. \quad (77)$$

The condition of the short-circuiting reads:

$$E_d d + N l_f E_f + N l_p E_p = 0. \quad (78)$$

This system of three linear equations has non-trivial solutions (point of the stability loss of the paraelectric phase) if

$$\varepsilon_f = -\frac{l_f \varepsilon_p}{l_p \left(1 + \frac{d \varepsilon_p}{N l_e}\right)} \simeq -\frac{l_f \varepsilon_p}{l_p}. \quad (79)$$

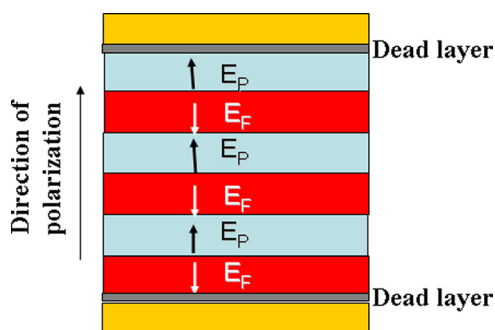


FIG. 15. (Color online) Schematic of a superstructure with real electrodes (denoted by the presence of dead layers at the oxide-electrode interfaces). The electric field in the paraelectric ( $E_p$ ) and in the ferroelectric ( $E_f$ ) are in opposite directions to satisfy  $D = \text{constant}$  in the system.

For sufficiently large  $N$ , the last approximate equality is almost exact even for very poor electrodes, i.e., those with large  $d$  and small  $\varepsilon_e$ . Physically, this means that even the presence or absence of the electrodes is not important for the phase transition into a single domain state.

But to define conditions for a single domain transition and to find the temperature and other characteristics of a phase transition into a multidomain state, one has to take into account the parameters of the electrodes as our paper convincingly shows. This is not, unfortunately, an easy task in realistic cases. It is also natural to expect that the difference between the first and second superstructures will be less dramatic than we have found in this paper if these superstructures are supplied with real electrodes. All in all, at the moment, we do not propose to carry our work further and take into account the real nature of the electrodes as we think that this question deserves a separate study.

## V. CONCLUSIONS

We considered the phase transition in superstructures consisting of ferroelectric-paraelectric units having equal layer thicknesses and the case where the polar axis is perpendicular to the film plane. Our aim was to find the phase transition temperature and the profile of the polarization appearing at the transition. To do so, we used the phenomenological Landau—Ginzburg—Devonshire theory together with the equations of electrostatics. The effects of non-electrostatic boundary conditions have been neglected. The approach was general but to illustrate the results we referred to the BaTiO<sub>3</sub>—SrTiO<sub>3</sub> system. The ferroelectric phase transition in the superstructures is known to be into a multidomain state if the thickness of the layers is larger than a certain (“critical”) thickness. For such transitions, we showed that the transition temperature and domain structures appearing at the transition are very sensitive to the nature of the near-electrode regions. Specifically, whether electrodes are in contact with the ferroelectric layers or not has a prominent impact on these characteristics as well as on the value of the critical thickness. Moreover, the typical situation proved to be that the amplitude of the appearing polarization “waves” in the plane of a given layer is a function of the layer position with respect to the electrodes. This is irrespective of the number of the units in the superstructure and, therefore, the usual assumption about periodicity in superstructures with sufficiently large number of units is not justified. The periodicity is possible in a special case only when the near-electrode layers are paraelectric with half layer thickness. This is once again valid irrespective of the number of the units and is connected with a symmetry that the whole structure has in this case. There are many types of inhomogeneous polarization distributions that should in principle be considered as candidates for the polarization distribution appearing at the phase transition. It proves unfeasible to find all these distributions even for systems with a small number of units, not to mention the general case. We were, however, able to find a type of polarization distribution that should be considered as the strongest candidate for the polarization at the transition if one of the electrodes is in direct contact

with the ferroelectric layer and the number of repeating units is arbitrary. The same is possible for the symmetrical superstructure mentioned in the preceding text. Using physical arguments, we have put forward a hypothesis that exactly these distributions appear at the phase transition in the respective superstructures. Our numerical simulations have supported this hypothesis. Note that the inherent inhomogeneity along the superstructure of the domain structures appearing at the phase transition should result in considerable smearing of the phase transition anomalies observed for multidomain transitions. This smearing is not present and the structure of the near electrode region is not felt for the single domain transition expected for thicknesses lower than the critical one. It should be recalled, however, that the value of the critical thickness does depend on the structure of the near electrode region.

## ACKNOWLEDGMENTS

A.P.L. has been partially supported by the Scientific and Technological Research Council of Turkey (TÜBİTAK) through the BİDEB Program and by the Ministry of Science and Education of Russian Federation (State Contract No. 02.740.11.5156). I.B.M. acknowledges the support of the Turkish Academy of Sciences (TÜBA) GEBİP Program.

<sup>1</sup>E. D. Specht, H. -M. Christen, D. P. Norton, and L. A. Boatner, *Phys. Rev. Lett.* **80**, 4317 (1998).

<sup>2</sup>D. A. Tenne, A. Bruchhausen, N. D Lanzillotti-Kimura, A. Fainstein, R. S Katiyar, A. Cantarero, A Soukiassian, V. Vaithyanathan, V. J. H. Haeni, W. Tian, D. G. Schlom, K. J. Choi, D. M. Kim, C. B. Eom, H. P. Sun, X. Q. Pan, Y. L. Li, L. Q. Chen, Q. X. Jia, S. M. Nakhmanson, K. M. Rabe, and X. X. Xi, *Science* **313**, 1614 (2006).

<sup>3</sup>D. Schlom, L. Q. Chen, C.-B. Eom, K. M. Rabe, S. K. Streiffer, and J.-M. Triscone, *Annu. Rev. Mater. Res.* **37**, 589 (2007).

<sup>4</sup>E. Bousquet, M. Dawber, N. Stucki, C. Lichtensteiger, P. Hermet, S. Gariglio, J.-M. Triscone, and P. Ghosez, *Nature* **452**, 732 (2008).

<sup>5</sup>N. A. Pertsev, P.-E. Janolin, J.-M. Kiat, and Y. Uesu, *Phys. Rev. B* **81**, 144118 (2010).

<sup>6</sup>J. Y. Jo, P. Chen, R. J. Sichel, S. J. Callori, J. Sinsheimer, E. M. Dufresne, M. Dawber, and P. G. Evans, *Phys. Rev. Lett.* **107**, 055501 (2011).

<sup>7</sup>K. K. Galipeau, P. P. Wu, Y. L. Li, L. Q. Chen, A. Soukiassian, X. X. Xi, D. G. Schlom, and D. A. Bonnel, *ACS Nano* **5**, 640 (2011).

<sup>8</sup>X. F. Wu, K. M. Rabe, and D. Vanderbilt, *Phys. Rev. B* **83**, 020104 (2011).

<sup>9</sup>Fishman, F. Schwabl, and D. Schenk, *Phys. Lett. A* **121**, 192 (1987).

<sup>10</sup>D. R. Tilley, *Solid State Commun.* **65**, 657 (1988).

<sup>11</sup>D. Schwenk, F. Fishman, and F. Schwabl, *Phys. Rev. B* **38**, 11618 (1988).

<sup>12</sup>D. Schwenk, F. Fishman, and F. Schwabl, *J. Phys. Cond. Mat.* **2**, 5409 (1990).

<sup>13</sup>K. Iijima, T. Terashima, Y. Bando, K. Kamigaki, and H. Terauchi, *J. Appl. Phys.* **72**, 2840 (1992).

<sup>14</sup>H. Tabata, H. Tanaka, and T. Kawai, *Appl. Phys. Lett.* **65**, 1970 (1994).

<sup>15</sup>J. B. Neaton and K. M. Rabe, *Appl. Phys. Lett.* **82**, 1586 (2003).

<sup>16</sup>A. L. Roytburd, S. Zhong, and S. P. Alpay, *Appl. Phys. Lett.* **87**, 092902 (2005).

<sup>17</sup>I. P. Batra and B. D. Silverman, *Solid State Commun.* **11**, 291 (1972).

<sup>18</sup>E. V. Chensky and V. V. Tarasenko, *Sov. Phys. JETP* **56**, 618 (1982); *Zh. Eksp. Teor. Fiz. Pis'ma Red.* **83**, 1089 (1982).

<sup>19</sup>V. A. Stephanovich, I. A. Luk'yanchuk, and M. G. Karkut, *Phys. Rev. Lett.* **94**, 047601 (2005).

<sup>20</sup>Y. L. Li, S. Y. Hu, D. Tenne, A. Soukiassian, D. G. Schlom, X. X. Xi, K. J. Choi, C. B. Eom, A. Saxena, T. Lookman, Q. X. Jia, and L. Q. Chen, *Appl. Phys. Lett.* **91**, 112914 (2007).

<sup>21</sup>We present the Chensky–Tarasenko method not following their paper literally but in a somewhat modernized form. They considered a vacuum dead layer. Other authors generalized their treatment, see e.g., A. S. Sidorkin, *Domain Structure in Ferroelectrics and Related Materials*, Cambridge Int. Science Publishing, (2006).

<sup>22</sup>H. Suhl, *Appl. Phys.* **8**, 217 (1975).

<sup>23</sup>A. Tagantsev, *Ferroelectrics* **375**, 19 (2008).

<sup>24</sup>A. M. Bratkovsky and A. P. Levanyuk, *J. Comp. Theor. Nanosci.* **6**, 1 (2009).

<sup>25</sup>N. A. Pertsev, A. G. Zembilgotov, and A. K. Tagantsev, *Phys. Rev. Lett.* **80**, 1988 (1988).